Systematic Literature Review on Methodology and Manufacturing Process of Personalized Tablet using Selective Laser Sintering Technology

Nurul Huda Kamsani¹, Muhammad Shamsuri Hasan¹, Bappaditya Chatterjee², Muhammad Salahuddin Haris¹*

1. Department of Pharmaceutical Technology, Kulliyyah of Pharmacy, International Islamic University Malaysia, Jalan Sultan Ahmad Shah, 25200 Kuantan, Pahang, Malaysia.
2. Shobhaben Pratapbhai Patel School of Pharmacy & Technology Management (SPPSPTM), SVKM's NMIMS, Mumbai, Maharashtra, INDIA.

Info Article	ABSTRACT
	Three-dimensional printing (3DP) technology has garnered interests as a novel candidate for future pharmaceutical manufacturing. Since the first drug product (Spritam®) has been approved for commercialization by the Food and Drug Administration (FDA), there has been an enormous opportunity for printing custom drugs using 3DP. Many 3DP methods have been documented for pharmaceutical applications in the literature. However, selective laser sintering (SLS) printing remains the least studied for pharmaceutical applications. There are many advantages and challenges in adopting an SLS method to fabricate personalized medicines, such as accurate, cheaper, and simpler ways to configure dosing for certain patient groups. In this study, we systematically reviewed all available literature investigating the technique of personalized printlets using SLS printing, and further discussed the method used in its process. A systematic searching strategy was performed in Scopus, PubMed, and Google Scholar databases using predetermined search strings. Of the 122 articles, only eight articles completely met the inclusion criteria, and they were subsequently used for data synthesis. The results showed that the printing process, spectrophotometry analysis, thermal analysis, X-ray powder diffraction and characterization of the printlet were the vital parameters in the printing method, leading to potential pharmaceutical applications in personalized medicine. **Keywords:** Three-dimensional printing (3DP); selective laser sintering; personalized medicine

INTRODUCTION

Additive manufacturing (AM) or three-dimensional printing (3DP) has provided an accurate, cheaper and simpler way to configure dosing for patients and other uses to tailor drugs to the need; it is formerly a complicated area and costly in pharmaceutical manufacturing (Khan *et al.*, 2019). The International Standard Organization (ISO) has defined 3DP as "fabrication of objects through the deposition of a material using a print head, nozzle, or another printer technology" (Jamróz *et al.*, 2018). 3DP technology has garnered interests as a novel candidate for future pharmaceutical manufacturing due to its benefits such as on-demand production, complex structure

manufacturing capacity, high precision droplet size control, precise distinct and specific geometries growth, accurate dosing, reproducibility, and cost-effectiveness (Khan *et al.*, 2019; Park *et al.*, 2019).

In 2015, the first 3DP drug Spritam® was introduced into the market as an epileptic drug, and it was produced with ZipDose® technology (Voelker, 2015). 3DP has continued to grow rapidly since then, with research highlighting the many new opportunities that the technology can provide. In order to test their suitability for pharmaceutical applications, researchers investigate and explore more 3DP technologies. This AM technology can be classified into seven groups: binder jetting (inkjet and aerosol 3D printing), directed energy

deposition, material extrusion (FDM, 3D dispensing, 3D fiber deposition, and 3D plotting), material jetting, powder bed fusion (SLS), sheet lamination, and vat photo-polymerization (stereolithography) (ASTM F2792-12a, 2012; Ligon *et al.*, 2017).

Selective laser sintering (SLS) is categorized under the powder bed fusion group which uses a laser beam to heat up powder particles and then, fuses them at their surfaces to create a designated solid object (Fina *et al.*, 2018a). First developed by Carl Deckard in 1984, the SLS technology is based on a neodymium-doped yttrium aluminum garnet (Nd:YAG) laser, which has a power of 100 W (Beaman and Deckard, 1990). The technology uses a thermoplastic polymer, namely acrylonitrile butadiene styrene (ABS) as the printer feedstock material in most designs (Shellabear and Nyrhilä, 2004). Many commercially produced SLS printers now use carbon dioxide (CO_2) lasers, which have higher strength at a lower cost, enabling the use of a wide variety of thermoplastic powder materials and making them more suitable for pharmaceutical application (Awad *et al.*, 2020). Although many studies have focused on the in-process parameters and methodology of SLS, there is yet a limited number of scholars who have reviewed the existing studies systematically. This systematic review was conducted in more details and with reproducible process (e.g., keywords used, articles selection). The review was guided by the central research question: What are the common methodology and manufacturing process of personalized tablets using SLS technology? This study aimed to fill the gap by reviewing previous related studies systematically to gain more understanding of the methodology and manufacturing process of personalized medicine, the parameters, and principles.

METHODOLOGY
The review protocol – PRISMA

Preferred Reporting Items for Systematic Literature Review and Meta-Analyses (PRISMA) is a published standard that guides researchers on systematic literature review. PRISMA is widely used in medical research, and it can identify the study's inclusion and exclusion criteria.

Formulation of the research question

The research question for this review was formulated based on PICo. PICo is an instrument that helps researchers to construct a pertinent research question for the systematic literature review. There are three main concepts in PICo: Population or Problem, Interest and Context. Based on the concepts, the researchers outlined three main aspects in the review: 3D Printing (Population), personalized tablet (Interest) and selective laser sintering (Context) which then guided the formulation of the main research question: What is the methodology and manufacturing process of personalized tablet using SLS technology?

Resources

The present review was carried out using two primary databases, namely Scopus and PubMed, due to their potential to be the leading databases in a systematic literature review (Mohamed Shaffril *et al.*, 2020a, 2020b, 2019). Both databases possess several advantages, such as the advanced searching function and a wide coverage of study disciplines, including 3DP and Pharmaceuticals, with the quality of the articles being highly controlled. For instance, Scopus indexes from over 5000 publishers that are rigorously vetted and selected by an independent review board while PubMed cites more than 30 million literatures, primarily focusing on health and health-related fields, including pharmaceuticals. Additionally, Google Scholar was chosen as the supporting database in the systematic review process for the advantages it provided, such as its ability to give vast results as there were over 389 million documents available in the database (Mohamed Shaffril *et al.*, 2020b).

Systematic searching strategies

The systematic searching process in selecting relevant articles for the present review was divided into three main stages: identification, screening, and eligibility.
Identification

During the first stage, the keywords were identified and then enriched by searching for similar or related terms using the dictionaries, thesaurus, and past research. The keywords were then connected by using a combination of symbols and coding, such as field codes, Boolean operators (AND, OR), wildcard, and truncation, to ease the searching process and narrow down the results to relevant articles (Mohamed Shaffril *et al.*, 2020b; Siddaway *et al.*, 2018). The search strings were developed (October 2020; refer Table I) and used on Scopus and PubMed after all keywords were determined. A total of 51 articles were retrieved from the two databases.

Table I. The search strings

Database	Search string
Scopus	TITLE-ABS-KEY (("Selective laser sinter*" OR "selective laser-sinter*" OR "SLS") AND ("3d print*" OR " three dimension* print*" OR "three-dimension* print*") AND ("personal* medicine" OR "personal* printlet" OR "individu* medicine"))
PubMed	(("Selective laser sinter*" OR "selective laser-sinter*" OR "SLS") AND ("3d print*" OR " three dimension* print*" OR "three-dimension* print*") AND ("personal* medicine" OR "personal* printlet" OR "individu* medicine"))
Google Scholar	allintitle: ("Selective laser sintering" OR "selective laser sintered" OR SLS) ("3d printing" OR " three-dimensional printer" OR "three-dimension printer")

Table II. The inclusion and exclusion criteria

Criterion	Inclusion	Exclusion
Literature type	Article journal (empirical data)	Systematic review, review papers, meta-synthesis, meta-analysis, conference proceedings, books, chapters in a book, book series
Language	English	Non-English
Timeline	2015 - 2020	<2015

As mentioned previously, Google Scholar was used as the supporting database and resulted in 71 articles. In total, 122 articles were identified in the first stage of the systematic searching process.

Screening

A total of 122 articles were automatically screened using the sorting function available in the databases by selecting the predefined inclusion and exclusion criteria (Table II). The first criterion decided was the type of the article, in which the researchers agreed to concentrate only on the research article due to their classification as the primary source and provision of empirical data (Mohamed Shaffril *et al.*, 2019; Siddaway *et al.*, 2018). Hence, publication in other forms than research articles, such as systematic review, review papers, meta-synthesis, meta-analysis, conference proceedings, books, chapters in a book, and book series, were excluded from the current review. Besides that, the current study only reviewed articles that were published in English. Thus, any publications in other languages were excluded. Moreover, the article's acceptable timeline to be included in the review was 6 years (2015-2020). However, as Google Scholar was only able to screen the timeline, manual screening was incorporated for the first two criteria. Overall, 66 articles did not meet the criteria (Table II) and they were excluded from the review. Along with the screening process, nine articles were found duplicated and were removed. The remaining 47 articles were retrieved and prepared for the next process: eligibility.

Eligibility

In the third stage, eligibility, the researchers manually examined the remaining 47 articles to ensure that they were fit to be included in the present study to achieve the study's objectives by thoroughly reading the articles' title and abstract. As a result, a total of 39 articles were omitted because of the emphasis on building anatomical replicas rather than medicine tablets, the focus on application in aiding surgery rather than tablet production, focus on manufacturing devices rather than tablets, comparison of different manufacturing methods, focus on polymer printability rather than a drug-excipient mixture, printability of different type of structure, and focus on physicochemical properties of printable. Overall, there were eight selected articles eligible for the next process: quality appraisal.

Quality appraisal

Quality appraisal was conducted to assess the quality of the articles' content. 73 articles were assessed by four authors individually and were ranked as high, medium, and low quality based on the predetermined criteria. The criteria were established based on the research questions of this systematic review. Mutual agreement between authors was practiced during the quality appraisal process to reduce the bias. The authors decided only to include high-quality articles for this study. Thus, eight articles proceeded with data abstraction and analysis (Figure 1).
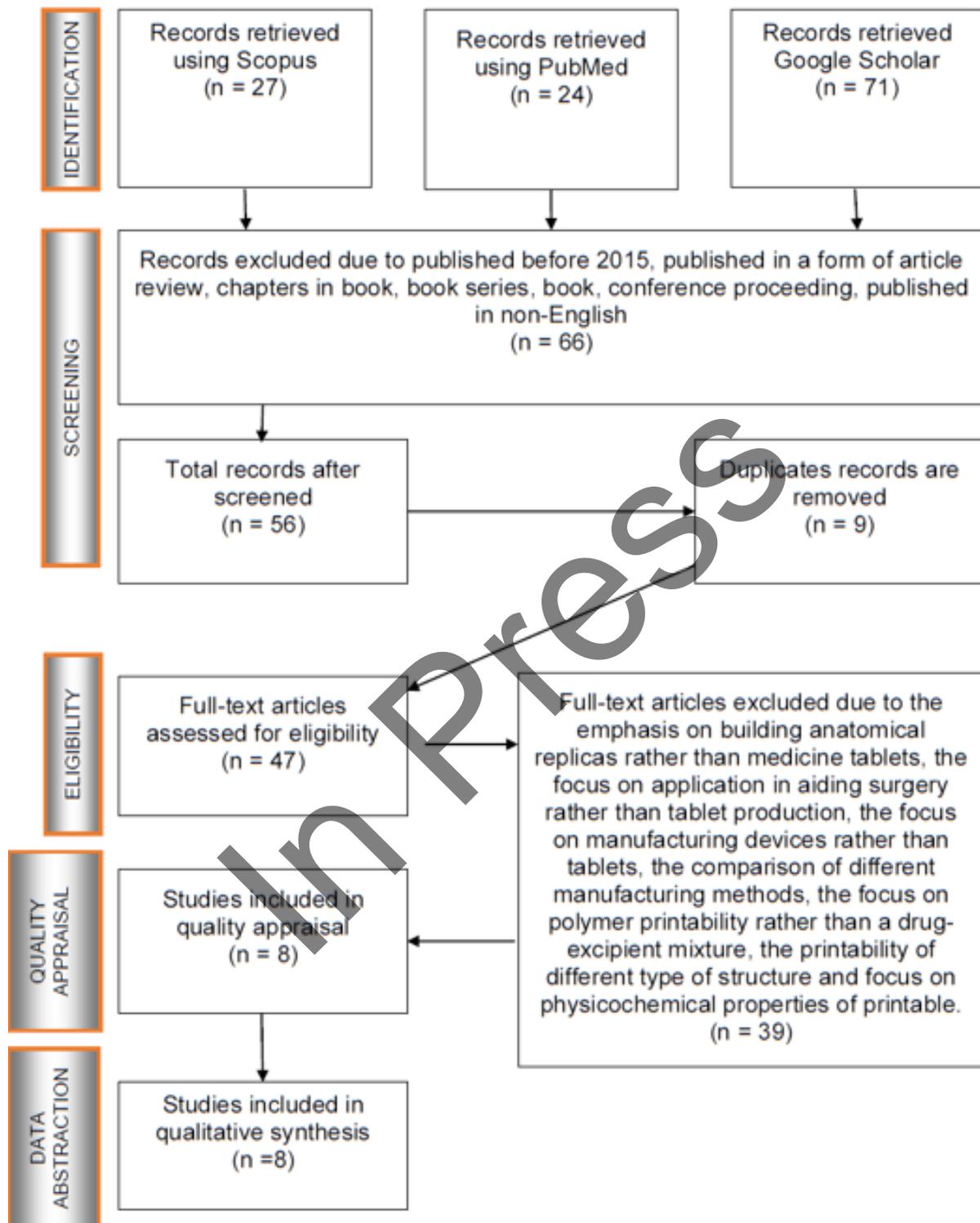
Figure 1. The Flow diagram of Systematic Literature Review (adapted from Mohamed Shaffril et al., 2019)

Data abstraction and analysis

The data abstraction was carried out based on the formulated research question. Any data from the reviewed research found capable of answering the research question were abstracted and tabulated. Next, thematic analysis was conducted to identify themes and sub-themes based on patterns, similarities, and relationships connecting the abstracted data.

The first step of the thematic analysis was to produce the themes. In this step, the researchers attempted to discover patterns that appeared connecting the abstracted data of all eight reviewed pieces of research. Any related or similar data were grouped, and eventually, a total of six themes were created. The researchers resumed the process on each created theme and further resulted in 12 sub-themes. Next, the researchers reviewed the data's accuracy and discussed with each other if there were any inconsistencies in the resulting themes and sub-themes to ensure the data's usefulness and accuracy. Afterwards, the researchers proceeded by naming the 6 themes: the printing process, spectrophotometry analysis, thermal analysis, X-ray powder diffraction, printlet (printed tablet) characterization and personalized medicine, and the sub-themes for each grouped data (Table III).

RESULTS AND DISCUSSION
Background of selected articles

The current review succeeded in obtaining eight selected articles. Six themes were developed based on the thematic analysis: printing process, spectrophotometry analysis, thermal analysis, X-ray powder diffraction, printlet characterization and personalized medicine. Twelve sub-themes also resulted in further study of the themes. Of the eight papers chosen, two were published in 2017 (Fina *et al.*, 2017; Salmoria *et al.*, 2017), two were published in 2018 (Fina *et al.*, 2018b, 2018a), two were published in 2019 (Awad *et al.*, 2019; Barakh Ali *et al.*, 2019) and two were published in 2020 (Allahham *et al.*, 2020; Trenfield *et al.*, 2020).

Themes and sub-themes
Printing process

Prior to powder use, 150-180 μm sieve has been used to ensure that suitable particle size was obtained for printing to enable the powder particles to flow better in the chamber and result in better printing process (Yap *et al.*, 2015). Using a mortar and pestle, 100 g of a mixture of drugs and excipients was mixed for all the formulations.

In order to enhance laser energy absorption and better printability, 3% Candurin® Gold Sheen was added to the formulation (Allahham *et al.*, 2020; Awad *et al.*, 2019; Barakh Ali *et al.*, 2019; Fina *et al.*, 2018b, 2018a, 2017; Trenfield *et al.*, 2020). The gold sheen added as the colorant made the prints appear yellow in color, and the powder particles were sintered and well connected in the region where the laser was targeted (Allahham *et al.*, 2020; Awad *et al.*, 2019; Barakh Ali *et al.*, 2019; Fina *et al.*, 2018b, 2018a, 2017).

The single miniprintlets were loaded with varying percentages of drugs used in the studies from 5-35% with a different ratio of drugs and polymers. In order to produce the oral dose formulations, powder mixtures were then transferred to a desktop SLS printer (Sintratec Package, AG, Brugg, Switzerland) (Allahham *et al.*, 2020; Awad *et al.*, 2019; Barakh Ali *et al.*, 2019; Fina *et al.*, 2018b, 2018a, 2017; Trenfield *et al.*, 2020). The 3D models were exported to the Sintratec central software 3D printer (Version 1.1.13, Sintratec, AG, Brugg, Switzerland) as stereolithography (.stl) format. Different types of software were used to design miniprintlet templates, such as 123D Design (Version 14.2.2, Autodesk Inc., San Rafael, CA, USA) to design spherical miniprintlet templates (1 mm and 2 mm in diameter) (Awad *et al.*, 2019). In contrast, AutoCAD 2014 (Autodesk Inc., USA) was used to design cylindrical form printlet templates which were about 10 mm diameter and 3.6 mm height (Fina *et al.*, 2018a, 2018b). Even though the shapes and structure were different, the diameter and height of the printlets were similar between different dosage forms.

Study conducted by Awad *et al.* (2019) showed that this technology managed to generate tablets that contained more than one drug. Other previous studies also showed successful development of modified-release tablets as well as immediate-release tablets (Barakh Ali *et al.*, 2019; Fina *et al.*, 2018a, 2017). The technology utilizes a thermal binding process to fuse powder particles together while the laser beam traces the 3D design by drawing a pattern on the powder bed (Fina *et al.*, 2018a; Shirazi *et al.*, 2015). Therefore, it is essential to understand the relationship of process parameters, particularly the surface temperature, chamber temperature, and scanning speed (Table IV) because these affect the quality characteristics of the printed dosage forms (Barakh Ali *et al.*, 2019).

Table III. The themes and sub-themes

Authors	Printing process (Powder)	Powder spectrophotometer analysis			Thermal analysis		X-ray Powder Diffraction (XRPD)	Characterization of printlets									Personalized medicine
		UVN	FTIR	NIR	DSC	TGA		MO	ST	FR	WV	SEM	XCT	DC	SO	IT	
Fina et al. (2018b)	✓	✓			✓		✓	✓				✓	✓	✓	✓	✓	✓
Fina et al. (2018a)	✓	✓			✓	✓	✓	✓				✓	✓	✓	✓	✓	✓
Fina et al. (2017)	✓	✓			✓	✓	✓	✓				✓	✓	✓	✓		✓
Trenfield et al. (2020)	✓		✓	✓	✓		✓	✓				✓	✓	✓	✓		✓
Barakh Ali et al. (2019)	✓		✓		✓	✓	✓	✓	✓			✓		✓	✓	✓	✓
Salmoria et al. (2017)	✓		✓		✓		✓	✓	✓			✓		✓	✓		✓
Allahham et al. (2020)	✓		✓		✓		✓	✓	✓		✓	✓		✓	✓	✓	✓
Awad et al. (2019)	✓							✓	✓		✓	✓		✓	✓	✓	✓

Powder spectrophotometer analysis
UVN – UV-Visible-near infrared
FTIR – Fourier transform infrared
NIR – Near-infrared

Thermal Analysis
DSC – Differential scanning calorimetry
TGA – Thermogravimetric analysis

Characterization of printlets
MO – Morphology
ME – Mechanical properties
ST – Strength
FR – Friability
WV – Weight variation
SEM – scanning electron microscopy
XCT – X-ray micro-computed tomography
DC – Drug content
SO – Dissolution test
IT – Disintegration test

Table IV. Summary of Surface temperature, Chamber temperature and Scanning speed from the literatures

Authors	Surface temperature (°C)	Chamber temperature (°C)	Scanning speed (mm/s)
Barakh Ali *et al.* (2019)	No data	115 to 135	270 to 330
Fina *et al.* (2018a)	50 to 120	35 to 100	No data
Trenfield *et al.* (2020)	40	30	200
Awad *et al.* (2019)	120	100	50
Salmoria *et al.* (2017)	45	open-air	350
Fina *et al.* (2017)	110	90	90
Fina *et al.* (2018b)	100 to 135	80 to 115	100-300 mm/s
Allahham *et al.* (2020)	100	80	200

Firstly, chamber or surface temperature effect is studied to ensure the printability of the dosage forms. This technology normally acquires high temperatures during the sintering process up to 135 °C. The study conducted by Barakh Ali *et al.* (2019) showed that if the temperature of the chamber was below 115 °C, the printlets did not develop successfully. However, if the chamber temperature was greater than 135 °C, the solidified powder-mixture matrix was generated in the reservoir. Besides that, the cylindrical and gyroid lattice printlets were successfully developed with different formulations of 92% polymers at a surface temperature of the powder bed during printing and chamber temperature ranging 50-120 °C and 35-100 °C, respectively (Fina *et al.*, 2018a). Another study reported suitability to print all the formulations with a chamber temperature of 90 °C and a surface temperature of 110 °C (Fina *et al.*, 2017). However, a study conducted by Trenfield *et al.* (2020) has proven otherwise since for the first time, printlets using low temperature SLS ranging 30-40 °C were developed, conferring benefits for heat-sensitive drugs or thermolabile drugs.

Another factor that can affect printlets weights and density is the laser scanning speed. A study conducted by Barakh Ali *et al.* (2019) observed that formulation with lower scanning speed of 270 mm/s would develop denser and higher weights of tablet of 257.0 ± 4.9 mg while higher laser scanning speed of 330 mm/s would develop less dense and more porous tablets weighted 214.3 ± 3 mg. Trenfield *et al.* (2020) have also shown a lower weight of tablet ranging between 162.6 ± 3.65 mg and 170.5 ± 10.8 mg with 200 mm/s scanning speed. This is because, the longer the period for powder particles to be exposed under low laser scanning speed, the greater the energy that will be absorbed during the sintering process. Consequently, this will lead to

reduction of empty spaces and more room filled by the sintered powder particles, creating more denser and heavier printlet (Awad *et al,* 2019; Fina *et al.*, 2018b, 2017).

Powder spectrophotometer analysis

Two studies employed UV–vis-NIR spectrophotometer Shimadzu UV-2600 in order to analyze the drug by measuring the absorbance in the solid state of the drug with or without excipients (Fina *et al.*, 2017; Trenfield *et al.*, 2020). The UV–Vis-NIR spectrophotometer Shimadzu UV-2600 measures wavelength between 220 and 1400 nm at room temperature (approximately 25 °C) using an integrating sphere as "Diffuse Reflectance Accessory (DRA)" (Fina *et al.*, 2017; Trenfield *et al.*, 2020). Next, the spectrophotometer analysis used mixtures of excipients, drugs, or mixtures with 0.5 g of barium sulphate and compressed them to form a disk of barium sulphate (Fina *et al.*, 2017). The results showed that the absorbance values tested at the same wavelength of the printer's blue diode laser (445 nm) were close to the baseline, suggesting that the laser light was not absorbed by the selected excipients, preventing the sintering process. Thus, adding Candurin® gold sheen at 3% w/w in the formulation was preferred due to its good degree of absorbance at 445 nm.

Another analysis used a non-destructive and non-invasive mobile Labspec 5000 NIR (Analytical Spectral Instruments, USA) benchtop spectrometer equipped with three separate holographic diffraction gratings and three separate detectors (Trenfield *et al.*, 2020). Then, 512-element silicon photo-diode array for wavelengths between 350 and 1000 nm and two Thermoelectric cooler indium gallium arsenide (TEC InGaAs) detector for wavelengths between 1000-1800 nm and 1800-2500 nm were used to test NIR reflectance (Trenfield *et al.*, 2020). All the prints have been scanned three times on each page.

Table V. HPLC parameters used to determine the drug content by the previous study.

Authors	Number of samples	Special dissolution requirement	Mobile phase	Column	Temperature	Flow rate	Sample injection volume	Sample detection
Fina et al. (2018b)	3 printlets	-	Methanol (15%) & Ultra water (85%)	C8 5 μm column, 250 × 4.6 mm	40 °C	1 mL/min	20 μL	λmax = 247 nm (PCM)
Fina et al. (2018a)	3 printlets	Ethylcellulose – Ethanol (due to insolubility) / Eudragit L100-55 – add 4 drops of NaOH (soluble at pH 5.5 and above)	Methanol (15%) water (85%)	and Ultra C8 5μm column, 25 × 4.6 mm	40 °C	1 mL/min	20 μL	λmax = 247 nm (PCM)
Fina et al. (2017)	3 printlets	Eudragit- 3 drops of 5N NaOH (dissolve at high pH)	Methanol (15%) water (85%)	and Ultra C8 5 mm column, 25 × 4.6 mm	40 °C	1 mL/min	20 μL	λmax = 247 nm (PCM)
Trenfield et al. (2020)	3 printlets	Deionised water and methanol (50:50)	Solvent A (HPLC water adjusted to pH 3 with phosphoric acid) and solvent (acetonitrile)*	Eclipse Plus C18 column (150 × 4.6 mm, B 5 μm particle size)	40 °C	1 mL/min	100 μL	λmax = 215 nm; Retention time: Amlodipine-1.9 min; Lisinopril-11.1 min
Awad et al. (2019)	20–25 mg miniprintlets from each size	of Kollicoat IR – water; Ethyl Cellulose – 10 ml methanol	Solvent A: acetonitrile and Solvent B: 0.1% formic acid in distilled water**	Eclipse plus C18 3.5 m column, 4.6 × 100 mm	40 °C	1 mL/min	20 μL	λmax = 230 nm; Retention time: Paracetamol – 2.57 min; Ibuprofen – 14.36 min
Allahham et al. (2020)	2 printlets from each formulation	HPLC water (100 mL)	Solvent A: NaH2PO4 buffer (30%) and Solvent B: Acetonitrile (70%)***	Eclipse Plus C18 5 μm, size: 250 × 4.6 mm	30 °C	1 mL/min	20 μL	λmax = 216 nm; Ondansetron

*Gradient elution with solvent A and solvent B ratio, 83:17 at t=0; 80:20 at t=6 min; 10:90 at t=15 min; 83:17 at t=18 min
**Gradient elution with 0-2 min, 15% A; 2–8 min, 15–55% A; 8–25 min, 55% A; 25–26 min, 55–15% A
***Gradient elution with 0 min: 100% mobile phase A; 20 min: 100% mobile phase B; 22 min: 100% mobile phase B; 23 min: 100% mobile phase A until 30 min

Table VI. Summary of dissolution test parameters

Author	Dissolution method	Apparatus	Dissolution condition	Buffer reagent	pH modulator	Temperature	Paddle speed	Detection device	Detection parameter
Fina et al. (2018b)	Dynamic dissolution	USP-II apparatus (Pharmatest PTWS)	Mimicking the stomach residence time (0.1M HCl), intestinal and colonic physiological environment medium (pH 5.6 decreasing to 7)	● Modified Hanks (mHanks) ● Modified Krebs (mKrebs) buffer	Auto pH System™ ●Carbon dioxide gas (pH increasing) ● Helium (pH decreasing)	37 ± 0.5 °C	50 rpm	in-line spectrophotometer	UV λmax = 247 nm (PCM)
Fina et al. (2018a)									λmax = 230 nm
Fina et al. (2017)									Retention time: Paracetamol – 2.57 min; Ibuprofen – 14.36 min
Awad et al. (2019)								HPLC	
Allahham et al. (2020)	Not stated		500 mL of 0.1 M HCl (USP monograph for ondansetron ODT)		N/A			in-line spectrophotometer	UV λmax = 310 nm
Salmoria et al. (2017)	Not stated	Dubnoff bath	50-mL phosphate buffer solution (pH:7.4)				Shaken: 60 rev/min	UV-visible spectrophotometer	λmax = 265 nm
Barakh Ali et al. (2019)	Not stated	USP apparatus 2 (Model 708-DS with 850-DS autosampler)	900 ml of 0.2M phosphate buffer (pH 6.8)				50 rpm	HPLC	λmax = 280 nm

1. mHanks buffer: (136.9 mM NaCl, 5.37 mM KCl, 0.812 mM $MgSO_4 \cdot 7H_2O$, 1.26 mM $CaCl_2$, 0.337 mM $Na_2HPO_4 \cdot 2H_2O$, 0.441 mM KH_2PO_4, 4.17 mM $NaHCO_3$)
2. mKrebs buffer: mHanks buffer + (400.7 mM $NaHCO_3$ and 6.9 mM KH_2PO_4)

The final spectrum which used to measure the content of amlodipine and lisinopril was recorded at six positions (6 average spectra/tablet). Using Microsoft Excel and MATLAB software version R2017a, the data was processed (The MathWorks, CA, USA). The wavelengths selected for lisinopril ranged between 1600 and 1730 nm while amlodipine ranged between 1450 and 1600 nm and 2000-2100 nm. Upon increasing the concentrations of both amlodipine and lisinopril formulations, there was an increase in the absorbance in NIR, suggesting their suitability for calibrating the generated model (Trenfield *et al.*, 2020).

In addition to that, two other studies used Fourier transform infrared (FTIR) along with NIR (near-infrared) (Barakh Ali *et al.*, 2019; Salmoria *et al.*, 2017). Sample spectrums from Fourier transform infrared (FTIR) were obtained using a modular Nicolet TM iSTM 50 system (Thermo Fisher Scientific, Austin, TX). The FTIR data collection parameters were: absorbance mode, wavenumber collected at range 400–4000 cm^{-1}, and data resolution at 8 cm^{-1} and 100 scans. Besides that, spectra capture, and analysis were performed using OMNIC software, version 9.0 (Thermo Fisher Scientific, Austin, TX). The chemical images of the printlets were obtained using the Via-Spec II Hyperspectral Imaging System, NIR (near-infrared). The images were collected from 900 to 2500 nm with SWIR hyperspectral camera (MRC-303–005-02, Middleton Spectral Vision, Middleton, WI) (Barakh Ali *et al.*, 2019).

Thermal Analysis

In order to characterize the powders and the drug-loaded into the printlets, thermal analysis is necessary. Differential Scanning Calorimetry (DSC) (six studies) and Thermogravimetric Analysis (TGA) (two studies) were the most common tests found. With a Q2000 DSC (TA instruments-Waters LLC, New Castle, DE, USA), DSC measurements were carried out at a temperature range of 0 °C to 200 °C, and a heating rate of 10 °C/min (2). Calibration for cell constant and enthalpy was performed with indium (T_m = 156.6 °C, ΔH_f = 28.71 J/g), as instructed by the manufacturer. For all the experiments, nitrogen was used as a purge gas with a 50 mL/min flow rate. TA Advantage software for Q series (Version 2.8.394) was used to collect the data and analyze by TA Instruments Universal Analysis 2000 (TA instruments—Waters LLC, New Castle, DE, USA). Unless otherwise mentioned, all melting temperatures were reported as an

extrapolated onset. TA aluminum pans and lids (T_{zero}) were used with an average sample mass of 3–5 mg.

For TGA, the average samples of 8-10 mg of raw drugs, polymers and powder mixtures were heated using a Discovery TGA (TA instruments-Waters LLC, New Castle, DE, USA) at a temperature range of 50 °C to 500 °C, and a heating rate of 10 °C/min in open aluminium pans. Nitrogen was used as a purge gas. The flow rate used was at 25 mL/min. The data were collected and analyzed using the TA Instruments Trios (Version 4.5.0.5) from which the percentage mass loss was measured with respect to temperature (Allahham *et al.*, 2020; Awad *et al.*, 2019; Fina *et al.*, 2018b, 2018a, 2017).

Before printing the printlets, DSC and X-ray analyses of the drug, polymers and mixed materials were conducted to determine the state of the drug and to what extent the drug was integrated into the polymers (Allahham *et al.*, 2020; Awad *et al.*, 2019; Fina *et al.*, 2018b, 2018a, 2017). A melting endotherm of drugs could be seen in the DSC data before printing. The melting endotherm, associated with the melting of the drug, can be found in the physical mixture of polymer powder mixtures, indicating that the drug is in its crystalline form.

Other than DSC as thermal analysis tools, Trenfield *et al.* (2020) added TGA for characterization. The stability of drugs has been determined by performing TGA characterization. Decomposition of lisinopril gradually occurred in three stages in which a dihydrate form of lisinopril by weight loss of ~8% up to 100 °C was observed. Secondly, there was no alteration in the dehydrated lisinopril crystal between 100 °C and 175 °C. The results in the last phase were similar with the previously reported literature in which the lisinopril crystal melted and degraded beyond 175 °C (Hinojosa-Torres *et al.*, 2008).

X-ray Powder Diffraction (XRPD)

The physical conditions of the drugs and the degree of their incorporation within the polymers were determined by X-ray Powder Diffraction method (Allahham *et al.*, 2020; Awad *et al.*, 2019; Barakh Ali *et al.*, 2019; Fina *et al.*, 2018b, 2018a, 2017). The majority of the studies used A Rigaku MiniFlex 600 (Rigaku, The Woodlands, TX, USA) with a Cu Kα X-ray source (λ = 1.5418 Å) and accompanying software Miniflex Guidance version 1.2.01 to record X-ray powder diffraction (XRPD) patterns. The applied intensity and voltage were 15 mA and 40 kV, respectively. The data acquisition

angular range was 3-40° 2θ, with a step size of 0.02° at a speed of 2° min^{-1} (Allahham *et al.*, 2020; Awad *et al.*, 2019; Fina *et al.*, 2018b, 2018a, 2017).

Another study by Barakh Ali *et al.* (2019) collected the XRPD patterns using a Bruker D2 Phaser SSD 160 Diffractometer (Bruker AXS, Madison, WI). The diffractometer was equipped with the LYNXEYE scintillation detector and Cu Kα radiation (λ=1.54184 Å) at a voltage of 30 kV and a current of 10 mA. The data collected were analyzed using Diffrac.EVA Suite (version V4.2.1) and further processed using File Exchange 5.0 (Bruker AXS, Madison, WI).

Corroborating the DSC findings, in all pure-polymers, physical mixtures and 3DP formulations for both polymers, the X-ray diffractograms demonstrated amorphous patterns. Furthermore, in the physical mixture, crystalline drug peaks were not observed as a 5% load could be too small for diffractograms to identify (Allahham *et al.*, 2020; Awad *et al.*, 2019; Fina *et al.*, 2018b, 2018a, 2017). However, a study by Allahham *et al.* (2020) showed that X-ray diffractograms did not provide clear evidence, and it could not be used to validate the DSC findings. Before and after printing, XRPD patterns of the formulations showed sharp peaks suggestive of a crystalline form of mannitol but did not provide essential information about the drug's state and how it was incorporated into the polymers.

Characterization of printlet

Printlets characteristics are crucial to determine the tablet acceptability, either by the regulators or consumers. The characteristics should fall within the acceptable limit set by the authorities through pharmacopeias, such as British Pharmacopeia (BP) and United States Pharmacopeia (USP). In this case, all eight previous studies were found to outline varying characterization techniques used in their study. Specifically, the determination of the morphology of the printlets was found in common under this theme (six studies), followed by the determination of printlet mechanical properties (seven studies), scanning electron microscopy (seven studies), X-ray micro-computed tomography (six studies), determination of printlet drug content (seven studies), dissolution test (seven studies) and disintegration test (three studies).

Determination of printlets morphology

The printlets diameter and thickness were determined using a digital calliper (Allahham *et al.*, 2020; Awad *et al.*, 2019; Barakh Ali *et al.*, 2019; Fina

et al., 2018b, 2018a, 2017). Awad *et al.* (2019) stated that the diameter measurement was made by averaging the diameters of 10 printlets. To determine the morphology of the printlets, images were taken using a digital camera to adequately describe the printlets appearance (Fina *et al.*, 2018b, 2018a), and the extra feature of the camera, such as macro-option, should be benefitted (Allahham *et al.*, 2020; Fina *et al.*, 2017). Besides printing tablets with ordinary shapes, constructing a gyroid lattice printlet (Fina *et al.*, 2018a) and multi-layered miniprintlet were also recorded (Awad *et al.*, 2019). Even though the shapes and structures were different, the diameter and height of the printlets were highly similar among the same formulation. The printlets appeared yellow due to the incorporation of Candurin® Gold Sheen in the formulation, which was used to help the sintering process (Allahham *et al.*, 2020; Awad *et al.*, 2019; Barakh Ali *et al.*, 2019; Fina *et al.*, 2018b, 2018a, 2017).

Determination of printlets mechanical properties

The mechanical properties determination techniques of the printlet were divided into three aspects: printlet strength, printlet friability and printlet weight variation. Firstly, for printlet strength, the printlet breaking force or hardness generally defines the strength of the printlets produced. The hardness of the printlets was determined using the traditional tablet hardness tester, TBH 200 (Erweka GmbH, Heusenstamm, Germany) (Allahham *et al.*, 2020; Fina *et al.*, 2018b, 2018a, 2017; Trenfield *et al.*, 2020) and tablet hardness tester VK 200 (Varian Inc, Cary, NC) (Barakh Ali *et al.*, 2019). The measurement was done by applying an increasing force perpendicular to the axis of the printlet until the printlet fractured.

Trenfield *et al.* (2020) stated that three printlets of each formulation were used to determine the hardness, and the mean and standard deviation of the data were used to represent the printlets collectively while Allahham *et al.* (2020) used six printlets as the samples. In general, an appropriate sample size should be predetermined for the test. The strength of the printlet will define the appropriate handling procedures of the printlet, and its resistance to breakage. Since some printlet might be pliable or deformed during the test, the hardness was unable to be measured (Fina *et al.*, 2018a, 2017; Trenfield *et al.*, 2020).

Apart from the tablet hardness tester, the quasi-static flexural test was also used for the

strength test by applying an oscillatory deformation onto the printlet (Salmoria *et al.*, 2017). The high flexural modulus and strength at 5% of elongation indicated greater printlet strength. Barakh Ali *et al.* (2019) and Fina *et al.* (2018b) stated that the laser scanning speed affected the strength of the printlets in a negative manner, whereby the strength of the printlet was reduced following an increase in the laser scanning speed. The contact time between the laser and the powder was shorter at higher scanning speed, thus lowering the impact of sintering and resulting in printlets with poor mechanical strength. On the contrary, higher laser energy will result in a stiffer printlet (Salmoria *et al.*, 2017). Moreover, the chamber temperature has shown a positive relationship with the printlet strength (Barakh Ali *et al.*, 2019). As the temperature increases, the degree of powder melt increases, thus more necks are formed within the printlet to confer its mechanical strength.

The next mechanical property is printlet friability. The friability of the printlets is defined as the percentage of weight loss over the original sample weight (Fina *et al.*, 2017; Trenfield *et al.*, 2020). Fina *et al.* (2017) and Trenfield *et al.* (2020) took approximately 6.5 g of printlets and three printlets of each different concentration as their sample, and placed the printlets into the friability tester, Friability Tester Erweka type TAR 10 (Erweka GmbH, Heusenstamm, Germany). The tester drum was spun at 25 rpm for 4 minutes or 100 rounds before the samples were reweighed. Ultimately, each previous study achieved friability of below than 1%, complying to the USP and BP requirement for uncoated tablets; thus, the printlets are suitable for handling and packing.

For the printlet weight variation, all of the printlets were weighed using a weighing balance, Sartorius AG CPA225D (Germany) (Trenfield *et al.*, 2020). For each printlet, the measurements were taken thrice, and the mean and standard deviation of the weights were calculated. Trenfield *et al.* (2020) managed to obtain less than 7.5% variation in printlets weight, which was considered as a pass according to the BP requirement. SLS produced printlets with highly similar weight (Allahham *et al.*, 2020; Awad *et al.*, 2019). Barakh Ali *et al.* (2019) explained that the laser scanning speed negatively affected while the chamber temperature positively influenced the printlet weight. The high scanning speed led to less effective sintering, consequently producing less dense printlets. On the contrary, the high chamber temperature will lead to a greater extent of sintering and in turn, produce denser printlets.

Scanning electron microscopy

Scanning electron microscopy (SEM) was employed to provide visual confirmation of the morphological characteristics of the printlets, the porosity of the printlets, laser effects on polymers and validation for X-ray micro–Computed Tomography (XµCT) results (Allahham *et al.*, 2020; Awad *et al.*, 2019; Barakh Ali *et al.*, 2019; Fina *et al.*, 2018b, 2018a, 2017; Salmoria *et al.*, 2017). The surface and cross-sectional images of the printlets were taken by using the scanning electron microscope, JSM-840A Scanning Microscope (JEOL GmbH, Germany) (Allahham *et al.*, 2020; Awad *et al.*, 2019; Fina *et al.*, 2018b, 2018a, 2017), JSM-7500F Scanning Electron Microscope (JEOL, Tokyo, Japan) (Barakh Ali *et al.*, 2019) and XL 30 Phillips microscope (Salmoria *et al.*, 2017). All researchers coated their samples with carbon up to 30-40 nm thick, except Salmoria *et al.* (2017), who coated their sample with gold using the Bal-Tec Sputter Coater SCD005. Barakh Ali *et al.* (Barakh Ali *et al.*, 2019) coated their sample using carbon, but only to approximately 5 nm thick using a sputter coater (Cressington, 208 HR with MTM-20 High-Resolution Thickness Controller) under high vacuum condition (argon gas pressure 0.01 mbar) and high voltage (40 mV). The images of the printlets were taken at a working distance of 15 mm, an emission current of 20 µÅ and an accelerated voltage of 5 kV. Barakh Ali *et al.* (2019) and Fina *et al.* (2018b) stated that the higher laser scanning speed would reduce sintering, leaving a more porous printlet. However, more porous tablets are not entirely disadvantageous as they facilitate liquid penetration and disintegrate faster, desired in orally disintegrating tablets (Allahham *et al.*, 2020).

Moreover, the use of high laser energy produces a printlet with extensive necks formed between the particles and co-continuous phases (Salmoria *et al.*, 2017). More molten areas seen in the images indicated more significant sintering impact in the materials (Fina *et al.*, 2017). In addition to that, the higher temperature also facilitates the sintering process, and leads to a closely packed and less porous printlet (Barakh Ali *et al.*, 2019). It should be noted that different active pharmaceutical ingredients (APIs) and polymer, and their composition will be sintered differently upon similar printing parameters. For example, the presence of fluorouracil (FU) in the polycaprolactone (PCL)/FU tablet results in a more

remarkable particle coalescence than the PCL tablet alone, which presumably is due to higher laser absorption by fluorouracil particles (Salmoria *et al.*, 2017), and the distinct region between the molten Ibuprofen/Ethyl Cellulose region and the Paracetamol/Kollicoat® IR sintered region seen in the dual miniprintlets (Awad *et al.*, 2019). A similar finding was also stated by Fina *et al.* (2017): the higher amount of paracetamol in both Eudragit L100-55 and Kollicoat® IR containing formulations produced a greater extent of molten areas of the printlet.

X-ray micro-Computed Tomography

X-ray micro-computed tomography (XμCT) is the technique employed to visualize the printlets' internal 3D structure and to determine their density and porosity (Allahham *et al.*, 2020; Awad *et al.*, 2019; Barakh Ali *et al.*, 2019; Fina *et al.*, 2018b, 2018a, 2017). All the previous studies used a similar high-resolution X-ray micro-computed tomography (XμCT) scanner, SkyScan1172 (Bruker-microCT, Belgium) with the resolution set at 2000 × 1048 pixels. The imaging process was done by rotating the printlets through 180° with steps of 0.4°, with four images taken at each step. The 3D image was then reconstructed using the NRecon software (Version 1.7.0.4, Bruker-microCT). The associate program CT-Volume software (Version 2.3.2.0) was used to render and view the 3D model. Then, the CT Analyzer software (Version 1.16.4.1) was used to analyze the collected data, and the density variation within the printlets was represented using different colors. The 3D analysis available in the morphometry preview was used to measure the porosity of the printlets, both closed and open porosity. Closed porosity is defined as "the pores of the printlet that do not extend to the external environment" whereas it is the otherwise for the open porosity; meanwhile, the total of both closed and open porosity yields the total porosity (Allahham *et al.*, 2020; Barakh Ali *et al.*, 2019; Fina *et al.*, 2018b). Printlet with greater open porosity was suggested to dissolve faster as the pores will be filled and in direct contact with the dissolution medium.

In contrast, closed porosity printlet dissolves slower than the equivalent structure of open porosity since the dissolution is mainly through erosion of the outer wall. On another occasion, Fina *et al.* (2018a) defined the porosity of a lattice printlet as "a mean of ten different individual sections at different heights of the printed structures with or without including non-printed spaces in the selection" and referred to the

non-printed spaces as an opening. It should be noted that the porosity increased significantly in printlets with openings. Besides that, the sintering effect was reduced at the higher scanning speed, resulting in less dense printlets (Fina *et al.*, 2018b). On another observations, the different compositions of the formulation affected the density of the printlets differently. For example, the Kollicoat® formulation was reported to have a similar total porosity with different drug (paracetamol) loading while the Eudragit formulation showed a reduced total porosity with increasing drug loading (Fina *et al.*, 2017). In dual miniprintlet, X-ray micro-CT distinguished the miniprintlet dual-configuration, and confirmed that the region did not mix during the sintering process (Awad *et al.*, 2019).

3.2.5.5. Determination of printlets' drug content

Determination of drug is crucial to determine the feasibility of SLS in printing 3D medication, aside from the safe and effective drug administration. Previous researchers performed qualification and quantification of the drug and its degradation metabolites, mainly using the high-performance liquid chromatography (HPLC) (Allahham *et al.*, 2020; Awad *et al.*, 2019; Fina *et al.*, 2018b, 2018a, 2017; Trenfield *et al.*, 2020) and UV-vis spectrophotometry (Salmoria *et al.*, 2017). Most of the researchers took three printlets from each formulation as their samples (Fina *et al.*, 2018b, 2018a, 2017; Trenfield *et al.*, 2020) while Allahham *et al.* (2020) only took two printlets from each formulation. Conversely, Awad *et al.* (2019) took 20-25 mg of the miniprintlets for the process, and Salmoria *et al.* (2017) took printlet segments from three different portions of the entire printlet produced. The HPLC parameters used by the previous researchers are tabulated in Table 5. Fina *et al.* (2018b, 2018a, 2017) reported that the detected paracetamol amount was highly similar to the theoretical loading dose in each separate study and confirmed that there was no degradation of paracetamol induced by SLS 3DP process. A similar finding was reported by Allahham *et al.* (2020): the quantified ondansetron drug loading by HPLC was very similar to the theoretical values, and the impurities recorded was below 0.2%, implying degradation of ondansetron did not occur. A small variation between the drug content and theoretical value may be explained by some degrees of variations in the drug distribution during the formulation and experimental procedures (Allahham *et al.*, 2020). On the other hand, Salmoria

et al. (2017) utilized the UV-vis spectrophotometry in their study to detect the amount of fluorouracil available in the printlet using the Hitachi 2010 double-beam UV-visible spectrophotometer at a wavelength of 265 nm.

Besides that, Trenfield *et al.* (2020) proposed a non-destructive dose verification technique for the 3D printed polyprintlets (printlets with more than one API) containing amlodipine and lisinopril. To measure the NIR reflectance for the procedure, they used a portable Labspec 5000 NIR spectrometer (Analytical Spectral Devices, USA), which was equipped with three separate holographic diffraction gratings and three separate detectors, a 512-element silicon photo-diode array (λ = 350 - 1000 nm), and two TE-cooled InGaAs (λ = 1000 - 1800 nm and 1800 - 2500 nm). For collecting spectra, an NIR equipment, BIF200-Vis-NIR (Ocean Optics Inc., FL, USA) with an attached immobilized laboratory-grade fibre optic cable (length 1 m; core size 200 µm), was used. The instrumental calibration was performed using the 99% reflective standard Spectralon (Labsphere, North Sutton, UK). Each printlet was scanned at six different spots, and all scans were performed three times on each side to minimize any possible sampling errors and variability due to the printlet surface, and a total of 64 scans were averaged. Using Microsoft Excel and MATLAB Central version 1.1.13, the resulting spectrum was averaged, and the data analyzed. For the calibration model development, Trenfield *et al.* (2020) took five oral films of different drugs concentrations (amlodipine 1-5% w/w & lisinopril 2-10% w/w) (25 samples) and two oral films from three different formulations for the internal validation (six samples). A multivariate analysis of the data was conducted using the MATLAB software version R2017a (The MathWorks, CA, USA), and the PLS Toolbox version 8.6 (Eigenvector, CA, USA) was utilized for data pre-processing and modelling. The calibration model was made using partial least squares (PLS) regression and was cross-validated internally using the Venetian blinds to evaluate the specificity, linearity (correlation coefficient, R2) and accuracy of the model (root mean square error of prediction, RMSEP). The procedure was conducted following guidance from Guidelines Q2(R1) of the International Conference on Harmonization (ICH), the Food and Drug Administration (FDA) and the European Medicines Agency (EMA). In the initial step of the calibration model development, pure drugs (amlodipine & lisinopril) and the polymer used, pure polyethylene oxide (PEO) 100000, were scanned to distinguish the individual peaks of interests (Trenfield *et al.*, 2020). The resulting NIR absorbance increased with the drug's concentration, suggesting the calibration curve development feasibility. Pre-treatment data was discovered to give better quantification accuracy. A technique was capable of detecting the well-known spectral features of amlodipine at 1450-1600 nm and 2000-2100 nm, and the well-known spectral features of lisinopril at 1600-1730 nm. The NIR showed excellent predictive performance for both drugs, amlodipine (RMSEP=0.24%) and lisinopril (RMSEP=0.24%) and showed no significant differences through the paired t-test with HPLC (p>0.05). A slightly higher error for amlodipine and lisinopril, RMSEP values of 0.26% and 0.7%, respectively, was recorded when the test was switched from thin film to cylindrical tablet. The error was supposed to be due to the cylindrical tablet's complex rounded shape, but ultimately, for tablets of similar composition, the model still fit for the purpose. In addition to being non-destructive, NIR is extremely user-friendly, and it can easily predict the dose (scanning time of roughly 10s).

Dissolution test

The dissolution test needs to be done to determine the drug release profile over time. The dynamic in-vitro dissolution test was famous among the previous studies, as it simulated the gastrointestinal tract's gastric and intestinal conditions (Awad *et al.*, 2019; Fina *et al.*, 2018a, 2018b, 2017). All of them were using the USP- II apparatus (Pharmatest PTWS 100, Germany) in the test. The printlets were placed in 750 mL of 0.1M HCl for 2 hours to mimic the gastric residence time and then transferred into 950 mL of modified Hanks's bicarbonate physiological medium for 35 minutes (pH 5.6 to 7) and into 1000 mL of Krebs buffer (pH 7 to 7.4, then to 6.5). The formulations were tested in the small intestinal environment (pH 5.6 to 7.4) for 3.5 hours and followed by the colonic environment (pH 6.5). The medium contains primarily bicarbonate buffers, in which bicarbonate and carbonic acid co-exist in equilibrium, along with aqueous CO_2 from carbonic acid dissociation. The buffer pH was controlled by an Auto pH System™. A pH probe supplies carbon dioxide gas and helium to reduce and raise the buffer's pH, respectively, controlled by the control unit, which dynamically adjusts the pH through the test and maintains pH uniformity over the unstable bicarbonate buffer pH. The USP-II apparatus's paddle speed was fixed at 50 rpm, and the tests

were carried out at 37 ± 0.5 °C for three replicates. The amount of drug released at any specific time was quantified using an in-line UV spectrophotometer (Fina *et al.*, 2018b) or HPLC (Awad *et al.*, 2019; Fina *et al.*, 2017). On the other hand, a simpler dissolution test was also preferable. Allahham *et al.* (2020) had their formulations tested using USP-II apparatus by placing them into 500 mL of 0.1 M HCl, as stipulated in the USP monograph for ondansetron orally disintegrating tablets (ODTs) while Barakh Ali *et al.* (2019) utilized the USP apparatus 2 (Model 708-DS with an 850-DS autosampler) and placed their formulations in 900 ml of 0.2M phosphate buffer (pH 6.8). Both of them retained similar paddle speed and temperature at 50 rpm and 37 ± 0.5 °C, respectively, and quantified the drug release using an in-line UV spectrophotometer (Allahham *et al.*, 2020) and HPLC system (Barakh Ali *et al.*, 2019) in a timely manner, and the measurements were done thrice. However, Salmoria *et al.* (2017) chose a different technique by using UV-Vis spectrophotometry in the test, immersed their dry specimen with known drug content into a 50-mL phosphate buffer solution (pH 7.4), and shook the sample in the Dubnoff bath at a rate of 60 revolutions per minutes to reduce the boundary effect. The measured absorbance at a wavelength of 265 nm was compared with the predetermined calibration curve to find the corresponding drug amount. The greater impact of sintering was associated with a slower dissolution rate (Barakh Ali *et al.*, 2019; Fina *et al.*, 2018b, 2017) and a more sustained drug release profile (Awad *et al.*, 2019).

Sintering at lower laser scanning speed will produce denser and more mechanically strong printlets, subsequently increasing the dissolution time (Barakh Ali *et al.*, 2019; Fina *et al.*, 2018b). This phenomenon is further explained by the porosity of the printlet; porous printlets have a greater exposed surface area and they are readily dissolved in the dissolution medium (Fina *et al.*, 2018b, 2018a). Fina *et al.* (2018a) highlighted that by enhancing the porosity of the printlets, the dissolution time was significantly shortened; even the Eudragit L enteric properties diminished in the lattice printlets (porous structure). Besides that, Barakh Ali *et al.* (2019) stated that the chamber temperature had a positive effect on the dissolution time, making the dissolution process longer. However, the dissolution test to compare fast disintegrating and dissolving formulations were considered not useful as the drug dissolved entirely in a very short duration (Allahham *et al.*, 2020;

Salmoria *et al.*, 2017).

Disintegration test

The disintegration test of the printlet was done to determine the duration required for the printlet to fully disintegrate in the medium. Previous studies outlined two main methods used: the petri dish method (Barakh Ali *et al.*, 2019; Fina *et al.*, 2018b), and the compendial method using USP disintegration apparatus (Allahham *et al.*, 2020; Barakh Ali *et al.*, 2019). According to Fina *et al.* (2018b), the petri dish method was based on the disintegration test for Spritam® (the first FDA-approved 3D printed medicine using powder bed technique). In this method, the printlets were placed in a petri dish containing 20 mL of water. Conversely, in the compendial disintegration test, one printlet was put in each tube of a basket containing 650 mL of water, and disks were put on top of the printlets (Allahham *et al.*, 2020). In both methods, the temperature was set at 37 ± 0.5 °C, mimicking the body temperature, and the time taken for the tablet to completely disintegrate was observed. There were six printlets from each formulation used in either method. Allahham *et al.* (2020) reported in their study that both of their formulations of ondansetron containing orally disintegrating printlet (ODP) disintegrated around 15 s, which were considered as an ODT according to the European Pharmacopoeia (EP) and the FDA. The higher porosity values suggest that the disintegrating media can enter the printlet structure readily and accelerate the disintegration process (Fina *et al.*, 2018b). In addition to that, the disintegrating time is reduced following an increasing laser scanning speed as higher laser scanning speed renders the printing process with less energetic sintering (Barakh Ali *et al.*, 2019; Fina *et al.*, 2018b). Subsequently, the powder particles of the printlet were allowed to disengage from each other upon contact with the disintegrating medium. By increasing the chamber temperature, the disintegrating time is also expected to increase as a denser and mechanically stronger printlet will be produced (Barakh Ali *et al.*, 2019).

Personalised medicine

It is highly advantageous to customize the dosage to the patient's needs by switching from "one-to-all" to personalized medicine. Several methods have been explored by previous studies to make this transition possible. Fina *et al.* (2018a) in their study investigated the geometry effects, namely cylindrical, gyroid lattice and cylindrical-

gyroid lattice bi-layer printlets, to the drug release profile. In general, the release of the drug from cylindrical printlets was highly dependent on the type of polymer used in the formulation. However, the gyroid lattice structure prints displayed a substantial decrease in the dissolution time due to the significant increase in exposed surface area and porosity. As the dissolution was amplified, the Eudragit L formulation with a gyroid lattice structure could not maintain its enteric properties and released most of the drug early in the dissolution test. Likewise, ethyl cellulose printlets released drugs four times faster than the cylindrical printlets. For the bi-layer printlets, the release was an intermediate between the cylindrical and gyroid lattice structure (Fina *et al.*, 2018a). The gyroid lattice structure contributed to the immediate burst of half of the drug loading while the remainder was sustainably released over time.

On the other hand, Fina *et al.* (2018b) demonstrated the feasibility of SLS in orally disintegrating printlet making. For those experiencing dysphagia, particularly pediatrics and geriatrics patients, this type of formulation is primarily beneficial. In this study, sintering using high laser scanning speed (v=300 mm/s) and less energetic sintering ultimately produced porous printlets with loose powder particles connections, which subsequently led to faster drug release. Similarly, shorter disintegration time was reported for the formulation of Kollidon® that sintered at 300 mm/s, with disintegration time being 4 s, satisfying the EP and FDA criteria for ODTs. Fina *et al.* (2018b) noted that SLS was a solvent-free method that did not require any subsequent drying after printing and therefore, was readily available to patients.

Allahham *et al.* (2020) also studied ODP, particularly on ondansetron containing ODP. This study altered the composition of the formulation, but no significant changes in the printlets and their disintegration time were observed. A low Kollidon VA-64 content (15% w/w) was found to be adequate for the printlet structure to be printed and maintained (Allahham *et al.*, 2020). This enables for the loading of more drugs into the formulation. Their printlets disintegrated completely in about 15 seconds. In addition to satisfying the ODT requirements, the time of disintegration was comparable to that of the commercial formulation (14.3 ± 2.7 s) (Allahham *et al.*, 2020).

Incorporation of more than one drug in a formulation was demonstrated by two studies,

amlodipine and lisinopril polyprintlets (Trenfield *et al.*, 2020), and paracetamol and ibuprofen dual miniprintlets (Awad *et al.*, 2019). However, Trenfield *et al.* (2020) focused on the non-destructive technique of dose determination of the polyprintlets in their study. Unlike Trenfield *et al.* (2020), whom incorporated amlodipine and lisinopril directly, Awad *et al.* (2019) produced dual miniprintlets with both drugs in different polymer at distinct region configurations (Configuration A: paracetamol mixed with Kollicoat IR (KIR) and ibuprofen with ethyl cellulose (EC); Configuration B: paracetamol mixed with ethyl cellulose (EC) and ibuprofen with Kollicoat IR (KIR)). Produced miniprintlets act as separate drug depot, in which both regions may contain different drug loading, and release the drug content through different mechanisms (Kollicoat – immediate release; ethyl cellulose – slow release) (Awad *et al.*, 2019).

Salmoria *et al.* (2017) manufactured an implantable anti-chondrosarcoma, PCL/FU printlet, through SLS. The implantable printlet showed no significant difference in the drug release profile following different intensity of sintering (laser sintering power – 3 and 7 W). The release of FU was high initially, which was desirable to provide high initial drug concentration in cancer tissues (Salmoria *et al.*, 2017). Subsequent slow and controlled release of the drug was to maintain the level of the drug at the target site. This profile is preferred since FU is capable of accumulating preferentially in the tumor cells.

The thematic analyses developed six themes and 12 sub-themes. This section presents further discussions of the developed themes, whereby in general, the fabrication of the ODPs has been successfully achieved (Allahham *et al.*, 2020; Awad *et al.*, 2019; Fina *et al.*, 2018b, 2018a, 2017). The printing process began with approximately 100 g of a drug mixture for all the formulations, and the excipients were mixed using a mortar and pestle. To enhance laser energy absorption and aid printability, 3% Candurin® Gold Sheen was added to the formulations (Allahham *et al.*, 2020; Awad *et al.*, 2019; Barakh Ali *et al.*, 2019; Fina *et al.*, 2018b, 2018a, 2017; Trenfield *et al.*, 2020). The gold sheen added as the colorant makes the printlets appear yellow, and the powder particles were sintered and well connected in the region where the laser was intended (Allahham *et al.*, 2020; Awad *et al.*, 2019; Barakh Ali *et al.*, 2019; Fina *et al.*, 2018b, 2018a, 2017). Without the use of the colorant, the powder would not absorb the light at the laser wavelength of the printer, rendering ineffective sintering.

There were no interactions between Candurin® gold sheen and the rest of the formulation components (Allahham *et al.*, 2020).

Asymmetrical and symmetrical stretching vibration bands at 1573 cm^{-1} and 1450 cm^{-1} were shown by powder spectrophotometer analysis for FTIR due to the carboxylate group while a distinct OH stretching vibration was at 3521 cm^{-1}. The presence of water molecules within the crystal lattice was suggested by this peak's shape and position. It also showed the characteristic doublet peaks corresponding to the C stretch skeletal vibrations at 1069 and 1030 cm^{-1}.

Next, the thermal analysis, DSC, TGA and X-ray tests of the drug, polymers and mixed materials prior to printing and of the printlets themselves were carried out to determine the drug's state and to what extent the drug was integrated into the polymers. The analysis was conducted before printing to indicate the existence of the drugs. If the printlet DSC data showed a broad melting endotherm prior to the drug melting endotherm temperature, the drug was either molecularly distributed as a solid dispersion within the polymer matrix or dissolved in the polymer as the temperature increased during the DSC experiment.

The characterization techniques available in the previous researches included determination of printlets morphology, determination of printlets mechanical properties, scanning electron microscopy, X-ray micro-computed tomography (XμCT), determination of printlets drug content, dissolution test, disintegration test and thermal analysis.

The first technique, determination of printlets morphology, provides the initial estimate on the acceptance of the drug-containing printlets by the consumers. According to the International Pharmacopeia, the tablets' requirements to pass the inspection are that the tablets should be undamaged, smooth, and uniform in color. Besides that, pediatric patients are more attracted to printlets with visually appealing characteristics (Januskaite *et al.*, 2020). Thus, crumbly, dry, and sandy appearing printlets may be unacceptable for this age group.

Second, the determination of printlet mechanical properties, like printlet strength and friability is mainly done to determine the appropriateness of printlets manipulation procedures, such as handling and packaging. Printlets should be able to withstand the mechanical forces put on them without losing their integrity (World Heath Organization, 2011). Some formulations, such as ODTs, do not require any minimum breaking force (Allahham *et al.*, 2020; Fina *et al.*, 2018b). Thus, having the orally disintegrating printlet packaged in individual blister packs would be tremendous and entirely accepted by the end-users.

The third technique is scanning electron microscopy. This technique helps the researchers to confirm the morphological properties of the printlets, their porosity, the extent of sintering, and the validation of the X-ray micro-computed tomography (XμCT). The extent of sintering, highly sintered printlet demonstrates more necks formation between the sintered printlet mixture particles.

Fourth, the X-ray micro-computed tomography (XμCT) is used to visualize the internal 3D structure of the printlets produced, and simultaneously determine their density and porosity. It is also useful to predict the disintegration and dissolution profile of the printlets. Fina *et al.* (2018a) stated that more porous and less dense printlets may facilitate the processes mentioned. In this technique, the density of the printlet may be represented in different colors or comparable in color and thus, it eases the evaluation process. Furthermore, X-ray micro-computed tomography also allows the researchers to calculate the porosity of the printlets.

Fifth is the determination of drug content. This technique is used to check the amount of drugs in the printlet and quantify any drug degradation metabolite to check the feasibility of SLS in printing the medication. Methods like high-performance liquid chromatography (HPLC) and UV-Vis spectrophotometry may provide the researchers with assurance on the suitability of the sintering process on the drugs since the degradation due to the sintering process is a significant concern (Allahham *et al.*, 2020). As most of the previous study recorded a highly similar printlet-drug content with the theoretical loading dose, it might suggest that no degradation was induced by the sintering process. However, a small degradation and variation in the content may occur, but it is justifiable due to some variations that occur during the whole process (from preparation until finished printing). Besides that, the non-destructive dose verification using near-infrared (NIR) spectrometry seems to give extra benefits (Trenfield *et al.*, 2020). This method has shown a comparable result with HPLC through the paired t-test result. However, further confirmation should be made since a slightly higher error was recorded

for different printlet geometry in a similar study.

The sixth technique is the dissolution test. In this test, the printlets' drug release profile can be obtained. This test may vary from a simple dissolution test to a dynamic dissolution test that simulates the gastric residence time and intestinal conditions. Proper paddling and shaking speed should be used to reduce the boundary effect of dissolution, and an appropriate temperature (T = 37 ± 0.5 °C) is necessary to closely simulate the body temperature. For the determination of drugs released at any specific time, similar apparatus used in determining the drug content is admissible. However, the dissolution test to compare orally disintegrating printlets may be considered meaningless since they disintegrate and dissolve really fast.

Lastly is the disintegration test. This test is solely done to investigate the required time for printlets to fully disintegrate. Interestingly, one of this technique's methods is based on the disintegration test of the first 3D printed orally disintegrating tablet, Spritam® (Fina *et al.*, 2018b). The other method is the compendial disintegration test. The methods may be done at a temperature of 37 ± 0.5 °C to simulate the human body's temperature. The European Pharmacopeia defines orally disintegrating tablets as those that disintegrate in less than 3 minutes. On the other hand, the Food and Drug Administration (FDA) only considers those that dissolve within 30 seconds upon contact with the disintegrating medium, including saliva. Thus, this test may be crucial to those who want to make orally disintegrating printlets.

In addition to that, several printing parameters were found to influence the characteristics of the printlets. The first parameter is the laser scanning speed. Higher laser scanning speed was observed to reduce the printlet strength and produce porous printlets. According to Goodridge *et al.* (2012), the laser scanning speed is the "velocity at which the laser beam travels as it traverses a scan vector" and it is one of the most significant and commonly altered parameters of the energy density equation (see *Equation 1*). High laser scanning speed will make the contact time between the laser and the powder shorter, thus reducing the impact of sintering on the powder. As high laser scanning speed produces more porous printlets, the disintegration medium can readily run through the printlet structure and speed up the disintegration process. In addition to that, the printlet also has a greater effective surface area for

the disintegration and dissolution to occur. Conversely, lower laser scanning speed results in more significant sintering impact and produces stronger and denser printlets. Extensive necks are formed between the powder particles (Salmoria *et al.*, 2017), further resulting in a slower dissolution rate and possibly rendering a sustained-release formulation.

$$\text{Energy Density (ED)} = \frac{LP}{SS \times BS} \, J/mm2 \dots \textbf{Equation 1}$$

Where, LP – laser power; SS – scan spacing; BS – laser scanning speed

The second parameter is the chamber temperature. The strength of the printlets increases with an increase in the chamber temperature. A similar effect is also recorded for the printlet weight, dissolution time and disintegration time. According to Barakh Ali *et al.* (2019), a rise in temperature increases the degree of powder melt, facilitates more necks formation within the printlets, and provides its mechanical strength. The greater extent of sintering with high chamber temperature, in turn, forms a denser and heavier printlet. As the resulting printlets were denser, fewer pores are formed within the printlets, consequently not allowing the disintegration medium to enter the printlet to expedite the process. The effective surface area of the printlets for disintegration and dissolution is less compared to more porous printlets. Practically, the bed and chamber temperature are often bounded by the SLS system used, usually around 200 °C for commercial devices (Goodridge *et al.*, 2012). However, this probably would not be an issue for pharmaceuticals since drugs may degrade at high temperatures, and degradation is detrimental in producing a safe and efficacious medication.

The extent of sintering is also influenced by the composition of active pharmaceutical ingredients (API) and polymers. Salmoria *et al.* (2017) demonstrated that fluorouracil's presence in their tablet formulation showed a greater extent of sintering if compared to the polymer, polycaprolactone, and alone. Fina *et al.* (2017) recorded that the higher incorporation of paracetamol in both formulations, Kollicoat® IR and Eudragit L100-55, produced more molten area and greater sintering impact. The difference in the impact of sintering was also demonstrated by the distinct region of molten ibuprofen/ethyl cellulose

and paracetamol/Kollicoat® IR in the dual miniprintlets formulation (Awad *et al.*, 2019). The sintering impact may differ from one polymer to another, thus suggesting that more studies need to be done to investigate the impact on different pharmaceutical-grade polymers and APIs.

On the other hand, the geometry of a printlet is crucial in assisting the dissolution and disintegration process. Fina *et al.* (2018a) demonstrated that the release of paracetamol from an Eudragit L lattice printlet resembled the release of an immediate-release tablet in the gyroid lattice structure. This suggests that the alteration of printlet geometry makes them more porous or increases the surface area, significantly altering their dissolution profile. Note that Eudragit L is a polymer used to formulate an enteric tablet.

Besides that, previous researchers managed to produce various types of printlets in their study. Fina *et al.* (2018a) altered their printlets to varying geometrical shapes, namely cylindrical, gyroid lattice and cylindrical-gyroid lattice bi-layer printlets. The drug release profile was significantly different in such alterations, with more porous printlets showing faster dissolution. SLS provides a straightforward approach to modify the drug release profile by altering the printlets geometry to fit the patient's needs. The same study also demonstrated the capability of SLS to manufacture printlets with multiple geometries (cylindrical-gyroid lattice bi-layer), which are able to finely tune the release profile, for example the initial burst and sustained release (Fina *et al.*, 2018a).

However, there were two studies on ODPs using different approaches. Fina *et al.* (2018b) used varying laser scanning speeds (100 – 300 mm/s) in their effort to produce an ODP. This study found that high laser scanning speed was capable of producing an ODP, signifying SLS in the production of ODPs. ODPs (generally ODTs) are highly beneficial to those who are having dysphagia, especially pediatrics and geriatrics, or are reluctant to swallow the medication, such as tablets and capsules (Fina *et al.*, 2018b). On the other hand, Allahham *et al.* (2020) tried altering their ODP formulation composition. However, such alteration did not produce any significant differences in the disintegrating time, consequently showing that the composition of the printlets did not affect the disintegration (at least in this study).

Interestingly, a low percentage of polymer (Kollidon IR) in the formulation of ondansetron containing ODP is printable and able to maintain the printlets structure (Allahham *et al.*, 2020). In such a manner, more APIs can be added to the formulation and potentially prolong the interval of administration if a similar case happens for sustained-release formulations, subsequently improving the patient compliance to the treatment.

Awad *et al.* (2019) and Trenfield *et al.* (2020) have highlighted the potential of SLS in printing polyprintlets. Incorporating more than one API in one printlet would be more beneficial to geriatrics as they are often associated with polypharmacy (multiple usages of medicines) in the treatment of pathologies and comorbidities (Haris *et al.*, 2020). SLS would be more beneficial since it can produce printlets with two distinct regions with different release profiles (Awad *et al.*, 2019). One region can have the immediate-release profile, releasing drugs intended for fast release. In contrast, the other region may release the drug in a sustained manner, providing the drug at the intended concentration over a period of time.

RECOMMENDATION

The present systematic literature review findings have led to several recommendations that may be useful for future researchers. First, future studies should emphasize in combining two or more drugs into one printlet. Drugs that are used in combination or indicated for chronic use should be prioritized in those studies. Next, the modifications of the printlet structure should vary, but at the same time appealing. Such modifications should not neglect the important characteristics that a printed tablet should possess. Furthermore, other printing parameters, like laser power and scan spacing, should be studied thoroughly to find more interesting effects they would render to the printlets.

On another note, it should be considered that the previous studies were focused only on few drugs, like paracetamol, amlodipine, lisinopril, ondansetron and fluorouracil, and few polymers, like Kollicoat® IR, Eudragit L, ethyl cellulose and others. Hence, more studies need to be done to investigate other drugs and pharmaceutical grade polymers' feasibility to be 3D printed using SLS technology.

CONCLUSION

The SLS process to develop personalized medicine interplay various manufacturing process and variables to produce high quality printlets with different formulation and structure geometries. Laser scanning speed, and surface and chamber temperature modulate different formulations of

printlets in terms of weight, disintegration time, hardness and dissolution. Non-destructive and non-invasive method such as FTIR, UV-vis-NIR and NIR are preferred technique in measuring dosage irrespective of the formulation design and composition. Lastly, SEM and X-ray micro-CT are important to visualize the conformation of the morphological properties of the printlets, the porosity of the printlets and laser effects on polymers. The review enables readers to have an overview on the manufacturing properties achieved by the SLS process so far to produce potential personalized medications.

ACKNOWLEDGEMENT

CONFLICT OF INTEREST

The authors declare no conflict of interest.

REFERENCES

Allahham, N., Fina, F., Marcuta, C., Kraschew, L., Mohr, W., Gaisford, S., Basit, A.W., Goyanes, A., 2020. Selective laser sintering 3D printing of orally disintegrating printlets containing ondansetron. Pharmaceutics 12. https://doi.org/10.3390/pharmaceutics12 020110

ASTM F2792-12a, 2012. ASTM F2792 - 12a Standard Terminology for Additive Manufacturing Technologies. https://doi.org/10.1520/F2792-12A

Awad, A., Fina, F., Goyanes, A., Gaisford, S., Basit, A.W., 2020. 3D printing: Principles and pharmaceutical applications of selective laser sintering. Int. J. Pharm. 586, 119594. https://doi.org/10.1016/j.ijpharm.2020.11 9594

Awad, A., Fina, F., Trenfield, S.J., Patel, P., Goyanes, A., Gaisford, S., Basit, A.W., 2019. 3D printed pellets (Miniprintlets): A novel, multi-drug, controlled release platform technology. Pharmaceutics 11. https://doi.org/10.3390/pharmaceutics11 040148

Barakh Ali, S.F., Mohamed, E.M., Ozkan, T., Kuttolamadom, M.A., Khan, M.A., Asadi, A., Rahman, Z., 2019. Understanding the effects of formulation and process variables on the

printlets quality manufactured by selective laser sintering 3D printing. Int. J. Pharm. 570, 118651. https://doi.org/10.1016/j.ijpharm.2019.11 8651

Beaman, J.J., Deckard, C.R., 1990. Selective Laser Sinterng With Assisted Powder Handlng. Google Patents. US4938816A.

Fina, F., Goyanes, A., Gaisford, S., Basit, A.W., 2017. Selective laser sintering (SLS) 3D printing of medicines. Int. J. Pharm. 529, 285–293. https://doi.org/10.1016/j.ijpharm.2017.06. 082

Fina, F., Goyanes, A., Madla, C.M., Awad, A., Trenfield, S.J., Kuek, J.M., Patel, P., Gaisford, S., Basit, A.W., 2018a. 3D printing of drug-loaded gyroid lattices using selective laser sintering. Int. J. Pharm. 547, 44–52. https://doi.org/10.1016/j.ijpharm.2018.05. 044

Fina, F., Madla, C.M., Goyanes, A., Zhang, J., Gaisford, S., Basit, A.W., 2018b. Fabricating 3D printed orally disintegrating printlets using selective laser sintering. Int. J. Pharm. 541, 101–107. https://doi.org/10.1016/j.ijpharm.2018.02. 015

Goodridge, R.D., Tuck, C.J., Hague, R.J.M., 2012. Laser sintering of polyamides and other polymers. Prog. Mater. Sci. 57, 229–267. https://doi.org/10.1016/j.pmatsci.2011.04. 001

Haris, M.S., Azlan, N.H.M., Taher, M., Rus, S.M., Chatterjee, B., 2020. 3D-printed drugs: A fabrication of pharmaceuticals towards personalized medicine. Indian J. Pharm. Educ. Res. 54, S411–S422. https://doi.org/10.5530/ijper.54.3s.139

Hinojosa-Torres, J., Aceves-Hernández, J.M., Hinojosa-Torres, J., Paz, M., Castaño, V.M., Agacino-Valdés, E., 2008. Degradation of lisinopril: A physico-chemical study. J. Mol. Struct. 886, 51–58. https://doi.org/10.1016/j.molstruc.2007.0 3.064

Jamróz, W., Szafraniec, J., Kurek, M., Jachowicz, R., 2018. 3D Printing in Pharmaceutical and Medical Applications – Recent Achievements and Challenges. Pharm. Res. 35. https://doi.org/10.1007/s11095-018-2454-x

Januskaite, P., Xu, X., Ranmal, S.R., Gaisford, S., Basit, A.W., Tuleu, C., Goyanes, A., 2020. I spy with my little eye: A paediatric visual preferences survey of 3d printed tablets. Pharmaceutics

12, 1–16. https://doi.org/10.3390/pharmaceutics12 111100

Khan, F.A., Narasimhan, K., Swathi, C.S.V., Mustak, S., Mustafa, G., Ahmad, M.Z., Akhter, S., 2019. 3D Printing Technology in Customized Drug Delivery System: Current State of the Art, Prospective and the Challenges. Curr. Pharm. Des. 24, 5049–5061. https://doi.org/10.2174/13816128256661 90110153742

Ligon, S.C., Liska, R., Stampfl, J., Gurr, M., Mülhaupt, R., 2017. Polymers for 3D Printing and Customized Additive Manufacturing. Chem. Rev. https://doi.org/10.1021/acs.chemrev.7b00 074

Mohamed Shaffril, H.A., Ahmad, N., Samsuddin, S.F., Samah, A.A., Hamdan, M.E., 2020a. Systematic literature review on adaptation towards climate change impacts among indigenous people in the Asia Pacific regions. J. Clean. Prod. 258, 120595. https://doi.org/10.1016/j.jclepro.2020.120 595

Mohamed Shaffril, H.A., Samah, A.A., Samsuddin, S.F., Ali, Z., 2019. Mirror-mirror on the wall, what climate change adaptation strategies are practiced by the Asian's fishermen of all? J. Clean. Prod. 232, 104–117. https://doi.org/10.1016/j.jclepro.2019.05. 262

Mohamed Shaffril, H.A., Samsuddin, S.F., Abu Samah, A., 2020b. The ABC of systematic literature review: the basic methodological guidance for beginners. Qual. Quant. https://doi.org/10.1007/s11135-020-01059-6

Park, B.J., Choi, H.J., Moon, S.J., Kim, S.J., Bajracharya, R., Min, J.Y., Han, H.K., 2019. Pharmaceutical applications of 3D printing technology: current understanding and future perspectives. J. Pharm. Investig. 49, 575–585. https://doi.org/10.1007/s40005-018-00414-y

Salmoria, G., Vieira, F., Ghizoni, G., Marques, M.,

Kanis, L., 2017. 3D printing of PCL/Fluorouracil tablets by selective laser sintering: Properties of implantable drug delivery for cartilage cancer treatment. Rheumatol. Orthop. Med. 2, 1–7. https://doi.org/10.15761/rom.1000121

Shellabear, M., Nyrhilä, O., 2004. DMLS – Development History and State of the Art. Lane 2004 1–12.

Shirazi, S.F.S., Gharehkhani, S., Mehrali, M., Yarmand, H., Metselaar, H.S.C., Adib Kadri, N., Osman, N.A.A., 2015. A review on powder-based additive manufacturing for tissue engineering: Selective laser sintering and inkjet 3D printing. Sci. Technol. Adv. Mater. 16. https://doi.org/10.1088/1468-6996/16/3/033502

Siddaway, A.P., Wood, A.M., Hedges, L. V., 2018. How to Do a Systematic Review: A Best Practice Guide for Conducting and Reporting Narrative Reviews, Meta-Analyses, and Meta-Syntheses. Annu. Rev. Psychol. 70, 747–770. https://doi.org/https://doi.org/10.1146/a nnurev-psych-010418-102803

Trenfield, S.J., Tan, H.X., Goyanes, A., Wilsdon, D., Rowland, M., Gaisford, S., Basit, A.W., 2020. Non-destructive dose verification of two drugs within 3D printed polyprintlets. Int. J. Pharm. 577. https://doi.org/10.1016/j.ijpharm.2020.11 9066

Voelker, R., 2015. News from the Food and Drug Administration. JAMA -The J. Am. Med. Assoc. 313, 1898. https://doi.org/10.1001/jama.2015.4799

World Heath Organization, 2011. Revision of monograph on tablets. Int. Pharmacop. Revis. Monogr. TABLETS Final text Addit. to Int. Pharmacopoeia 1–6.

Yap, C.Y., Chua, C.K., Dong, Z.L., Liu, Z.H., Zhang, D.Q., Loh, L.E., Sing, S.L., 2015. Review of selective laser melting: Materials and applications. Appl. Phys. Rev. https://doi.org/10.1063/1.4935926